Terpsichorean Movements of Pentaammineruthenium on Pyrimidine and Isocytosine Ligands

Kathleen J. LaChance-Galang,[†,‡] Ishael Maldonado,[†] M. Louise Gallagher,[†] Wei Jian,[†] Alfred Prock,[§] Jerome Chacklos,[†] Roy D. Galang,[†] and Michael J. Clarke*[,†]

Merkert Chemistry Center, Boston College, Chestnut Hill, Massachusetts 02467, Department of Chemistry, Regis College, Weston, Massachusetts 02493, and Department of Chemistry, Boston University, Boston, Massachusetts 02215

Received May 12, 2000

Pentaammineruthenium moves on ambidentate nitrogen heterocycles by both rotation and linkage isomerization, which may affect the biological activity of potential ruthenium metallopharmaceuticals. The rapid rotation rates of $[(NH_3)_5Ru^{III}]$ coordinated to the exocyclic nitrogens of isocytosine (ICyt) and 6-methylisocytosine (6MeICyt) have been determined by ^1H NMR. Since these rotamers can be stabilized by hydrogen bonding between the coordinated ammines and the N1 and N3 endocyclic nitrogens, rotamerization is under pH control. Spectrophotometrically (UV−vis) measured pK_a values for the two endocyclic sites for the ICyt complex are 2.78 and 9.98, and for 6MeICyt are 3.06 and 10.21, which are probably weighted averages for ionization from N3 and N1, respectively. Activation parameters for the rotamerizations were determined by variable-temperature NMR at $pK_{a1} < pH < pK_{a2}$ for the complexes with $(ICyt^-\kappa^{N2})^-$, $(6MeICyt\kappa^{N2})^-$, and $2AmPym\kappa^{N2}$. For $[(6MeICyt\kappa^{N2})^-(NH_3)_5Ru^{III}]^{2+}$, $\Delta H^* = 1.6$ kcal/mol, $\Delta S^* = -37$ cal/mol K, and $E_a = 2.2$ kcal/mol. Due to strong $Ru^{III}-N$ π-bonding, the activation enthalpies are approximately 10 kcal lower than the expected values for the free ligands. Rotameric structure is correlated with pK_a values, pH-dependent reduction potentials, and ^1H NMR parameters. Linkage isomers of $[(2AmPym)(NH_3)_5Ru]^{n+}$ are reported in which Ru^{II} is coordinated to the endocyclic nitrogen (N1) and Ru^{III} to the exocyclic nitrogen (N2). The rate constant for the $\kappa^{N2} \rightarrow \kappa^{N1}$ isomerization as part of an ECE mechanism is 3.9 s^{-1} at pH 3. The pH dependence of the acid-catalyzed hydrolysis of $[(2AmPym\kappa^{N1})(NH_3)_5Ru]^{2+}$ is determined.

Introduction

Linkage isomerization and rotamerization occurs in some transition metal complexes of biological interest[1] and can affect their biological activity.[2] A number of ruthenium complexes with am(m)ine and imine ligands have exhibited good anticancer activity[3,4] with one currently in clinical trials.[5] Many of these complexes appear to exert their biological activity by affecting DNA metabolism, and the toxicity of some have been correlated with binding to nucleic acids in the cell nucleus.[6] Recently, we have shown that glutathione can reduce ammineruthenium coordination to N7-guanine sites (G^7) on DNA, but leave binding to the exocyclic nitrogens of adenine and cytosine relatively unaffected.[7]

Complexes of pentaammineruthenium(II/III) involving an exocyclic amine adjacent to an endocyclic imine, such as adenine and cytosine, can exhibit two types of metal ion movement: (a) linkage isomerization, in which the Ru^{III} is bound to the ionized exocyclic amine, while Ru^{II} coordinates to the adjacent endocyclic imine;[8] and (b) rotamerization, in which $[(NH_3)_5Ru^{III}]$ coordinated to the exocyclic amide rotates around the N−C bond.[9] A similar exo−endo (N1−N6) linkage isomerization has recently been reported with $(dien)Pt^{II}$ on adenosine (dien = diethylenetriamine).[10,11] Picolinamide complexes of the type $[L(NH_3)_5Ru^{II}]$, where L = nicotinamide or isonicotinamide, undergo linkage isomerization between the amide and pyridine nitrogens with specific rates of about 10 s^{-1},[12] while 2-picolinamide forms a chelate with Ru^{II} utilizing both nitrogens.[13,14] Linkage isomerization in an analogous glycine complex also illustrates that Ru^{II} prefers (softer) N-coordination while Ru^{III} prefers (harder) O-binding.[15]

We have used the term *terpsichorean* to describe complexes in which multiple metal ion movements can be controlled in a concerted fashion. For example, $[(NH_3)_5Ru^{III}]$ coordinates strongly to the deprotonated exocyclic amine of adenosine,

[†] Boston College.
[‡] Regis College.
[§] Boston University.

(1) Shoup, R. R.; H. T., M.; Becker, E. D. *J. Phys. Chem.* **1972**, *76*, 64−70.
(2) Skov, K. A.; Farrell, N. P. *Int. J. Radiat. Biol. Relat. Stud. Phys. Chem. Med.* **1987**, *52*, 289−97.
(3) Clarke, M. J.; Zhu, F.; Frasca, D. *Chem. Rev.* **1999**, *99*, 2511−33.
(4) Pieper, T.; Borsky, K.; Keppler, B. K. *Top. Bioinorg. Chem.* **1999**, *1*, 171−99.
(5) Sava, G.; Alessio, E.; Bergamo, E.; Mestroni, G. *Top. Biol. Inorg. Chem.* **1999**, *1*, 143−70.
(6) Clarke, M. J.; Frasca, D.; Ciompa, J.; Emerson, J. DNA binding and HeLa cell toxicity of antitumor ruthenium complexes. *Abstracts of Papers*, 211th National Meeting of the American Chemical Society, New Orleans, LA, March 24− 28, 1996; American Chemical Society: Washington, DC, 1996.
(7) Frasca, D.; Clarke, M. J. *J. Am. Chem. Soc.* **1999**, *121*, 8523−32.
(8) Clarke, M. J. *J. Am. Chem. Soc.* **1978**, *100*, 5068−75.
(9) Clarke, M. J. *Prog. Clin. Biochem. Med.* **1989**, *10*, 25−39.
(10) Arpalahti, J.; Klika, K. D.; Sillanpaa, R.; Kivekas, R. *J. Chem. Soc., Dalton Trans.* **1998**, 1397−402.
(11) Arpalahti, J.; Klika, K. D. *Eur. J. Inorg. Chem.* **1999**, 1199−201.
(12) Chou, M. H.; Brunschwig, B. S.; Creutz, C.; Sutin, N.; Yeh, A.; Chang, R. C.; Lin, C. T. *Inorg. Chem.* **1992**, *31*, 5347−8.
(13) da Rocha, Z. N.; Chiericato, G., Jr.; Tfouni, E. *Adv. Chem. Ser.* **1997**, *253*, 297−313.
(14) Rocha, Z. N.; Chiericato, G. Jr.; Tfouni, E. *Inorg. Chem.* **1994**, *33*, 4619−20.
(15) Diamond, S. E.; Taube, H. *J. Am. Chem. Soc.* **1975**, *97*, 5921−3.

10.1021/ic000512e CCC: $20.00 © 2001 American Chemical Society
Published on Web 12/28/2000

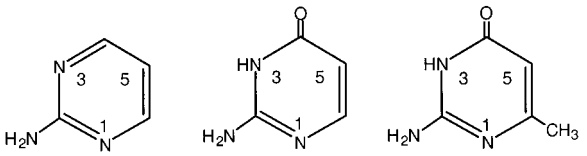

Figure 1. Structures of 2-aminopyrimidine (2AmPym) and one of the two tautomeric forms of isocytosine (ICyt) and 6-methylisocytosine (6MeICyt).

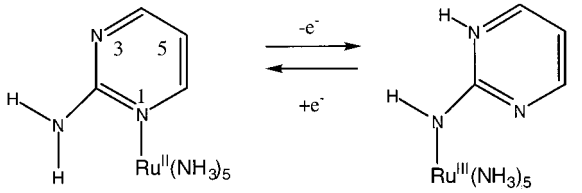

Figure 2. Redox-dependent linkage isomerization of $[(2AmPym\kappa^{N1})(NH_3)_5Ru^{II}]^{2+}$ and $[(2AmPym\kappa^{N2})(NH_3)_5Ru^{III}]^{3+}$.

where stabilization is provided by strong π-donation from the p-orbital of the nitrogen into a partially filled d_π-orbital on the metal ion resulting in a short Ru−N bond.[16,17] Following reduction to Ru^{II}, the metal ion moves to the adjacent pyrimidine ring nitrogen, where back-bonding interactions stabilize the lower-valent state. Movement back to the original site is possible upon oxidation, which greatly increases the acidity of the nearby exocyclic amine protons, thereby allowing facile displacement by Ru^{III}.[8] Rotamerization around the exocyclic N−C axis is pH-dependent. At neutral pH, an anionic charge resides on the pyrimidine ring, which promotes hydrogen bonding to N1. At lower pH, where N1 is protonated, weaker hydrogen bonding to N7 becomes favored causing the metal ion to swing to the opposite side of the molecule.[8,18]

In the present work, linkage isomers of $[2AmPym(NH_3)_5Ru]^{n+}$ (see Figures 1 and 2) were prepared and the rotamerization of $[(NH_3)_5Ru^{III}]$ around the exocyclic amines in 2-aminopyrimidine (2AmPym), isocytosine (ICyt), and 6-methylisocytosine (6MeICyt) was studied by NMR. The rate constant for the $\kappa^{N2} \rightarrow \kappa^{N1}$ isomerization as part of an ECE mechanism has been determined at a single pH. The rate of the acid-catalyzed hydrolysis of $[2AmPym(NH_3)_5Ru]$ was studied as a function of pH.

Experimental Section

Isocytosine (ICyt) was purchased from Sigma, and 2-amino-4-hydroxy-6-methylpyrimidine (6-methylisocytosine, 6MeICyt), and 2-aminopyrimidine (2AmPym) were purchased from Aldrich and used without further purification. $[Cl(NH_3)_5Ru]Cl_2$ was synthesized by literature methods.[19,20] $[Cl(NH_3)_5Ru](CF_3CO_2)_2$ was prepared by removal of the ionic chlorides from $[Cl(NH_3)_5Ru]Cl_2$ with $Ag(CF_3CO_2)$.

The compound $[(ICyt)(NH_3)_5Ru](ClO_4)_3$ was synthesized by reducing $[Cl(NH_3)_5Ru](CF_3CO_2)_2$ in the presence of a 10% excess of the ligand at pH 7 over zinc amalgam under argon for 45 min. The zinc was removed from the greenish-yellow solution, and the mixture was oxidized with air bubbling for 1 h, which resulted in a red solution. Following filtration, the reactant solution was chromatographed on an SP-Sephadex column, and the red band eluted with 0.4 M ammonium formate, which was removed by rotary evaporation. The residue was dissolved in a minimum of water, and a saturated solution of $NaClO_4$ in absolute ethanol was added to induce precipitation. The solution was cooled for ~2 h at 0 °C, to yield a reddish-purple powder, which was collected by filtration and washed with absolute ethanol. Yield: 70%. Anal. Calcd for $H_{20}C_4N_8O_{13}Cl_3Ru$: C, 8.06; H, 3.39; N, 18.81. Found: C, 7.71; H, 3.70; N, 18.85. UV−visible, λ_{max} (nm): 287, 370 (sh), 456. ^{1}H NMR (δ, ppm): −20.3 H5; −11.5, H6. pK_a: 2.78 ± 0.01 (N3), 9.98 ± 0.01 (N1). $E°$ (pH 2 vs NHE): 0.14 V.

The compound $[(6MeICyt)(NH_3)_5Ru](ClO_4)_3$ was prepared in the same way as $[(ICyt)(NH_3)_5Ru](ClO_4)_3$. While the elemental analyses of solid samples of the 6MeICyt complex were not within acceptable limits, electrospray mass spectra revealed the expected ruthenium isotope patterns with the parent peak for $[(6MeICyt^{2-})(NH_3)_5Ru]^+$ at 310 *m*/*e*, and the subsidiary patterns due to the loss of ammonia at 293, 276, 259 and 242 *m*/*e*. A set of peaks was also evident at 332 *m*/*e* for $[NaC_5H_{29}N_8Ru]^+$. For most studies, the complexes were used immediately after chromatographic purification. Isosbestic points were observed in the pK_a determinations. UV−visible, λ_{max} (nm): 290, 370 (sh), 470. ^{1}H NMR (δ, ppm): −20.3 H5; −11.5, CH_3. pK_a: 3.06 ± 0.01 (N3), 10.21± 0.02 (N1). $E°$ (pH 1.8 vs NHE): 0.10 V.

The compound $[(2AmPym\kappa^{N1})(NH_3)_5Ru](PF_6)_2$ was prepared by allowing 0.34 mmol of $[(H_2O)(NH_3)_5Ru]^{2+}$ to react with 0.68 mmol of 2-aminopyrimidine for 40 min under argon at pH 3−4 in approximately 3 mL of solution. A few drops of an argon-purged, concentrated solution of NH_4PF_6 were added to precipitate the product as an orange powder, which was washed with absolute ethanol. Yield: 78%. Anal. for $[(2AmPym\kappa^{N1})(NH_3)_5Ru](PF_6)_2$: Calcd: H, 3.53; C, 8.41; N, 19.61. Found: H, 3.34; C, 8.18; N, 19.11. UV−visible, λ_{max}, ϵ (M^{-1} cm^{-1}): in 1.0 M LiCl, 278 nm (3530 M^{-1} cm^{-1}), 440 nm (2840 M^{-1} cm^{-1}); in 1 M HCl, 293 nm (3160 M^{-1} cm^{-1}), 555 nm (2870 M^{-1} cm^{-1}). pK_a = 1.79 ± 0.05. The oxidized form of this complex was obtained as $[(2AmPym\kappa^{N2})^-(NH_3)_5Ru^{III}]Br_2$ by adjusting a solution of $[(2AmPym\kappa^{N1})(NH_3)_5Ru]^{2+}$ to pH 7 with dilute ammonia, bubbling oxygen through for at least 2 h, and then allowing the solution to stand in a refrigerator overnight. After filtering, the solution was placed onto a CM-Sephadex ion exchange column, which was eluted with 0.2−0.3 M ammonium formate before eluting the band with 0.5 M buffer. The desired fraction was rotary evaporated to remove the buffer. After dissolving the residue in a minimum of water, the solid product was obtained by adding a saturated solution of LiBr in ethanol. Anal. Calcd for $[(2AmPym\kappa^{N2})^-(NH_3)_5Ru^{III}]Br_2 \cdot 2H_2O$: H, 4.86; C, 10.09; N, 23.53; Ru, 21.2. Found: H, 4.53; C, 10.01; N, 23.68; Ru, 22.1. UV−visible, λ_{max}, ϵ (M^{-1} cm^{-1}): μ = 0.1 LiCl at pH 2, 234 nm (6010 M^{-1} cm^{-1}), 314 nm (6280 M^{-1} cm^{-1}), 454 nm (3950 M^{-1} cm^{-1}); at pH 7, 220 nm (6625 M^{-1} cm^{-1}), 260 nm (2291 M^{-1} cm^{-1}), 318 nm (4460 M^{-1} cm^{-1}), 515 nm (3812 M^{-1} cm^{-1}). ^{1}H NMR (δ, ppm): pH 1.5, 27.0, 21.0 H4 and H6; pH 7.5, 40 H4 and H6 (equivalent). pK_a = 4.94 ± 0.04. $[Pym(NH_3)_5Ru]Cl_2$ was prepared by published methods.[21] Its pK_a was determined spectrophotometrically as −0.18 ± 0.02.

Instrumentation. NMR spectra were obtained on Varian XL 300 and Unity 300 spectrometers. Sample sizes were 10−15 mg dissolved in 0.5 mL of D_2O placed in 5 mm NMR tubes previously dried in a 110 °C oven. The pH was adjusted with dilute solutions of DCl and NaOD and was not corrected for the isotope effect. UV−vis data were obtained on a Cary 2400 spectrophotometer. pK_a studies were performed by spectrophotometric titration at an ionic strength of 0.1 M LiCl.

Electrochemistry was performed in 0.1 M LiCl using a potentiostat interfaced with an IBM-AT running ASYST programs, constructed in this laboratory, or on a BAS 100A. The working electrode was carbon paste, the reference electrode was Ag/AgCl, and the counter electrode was platinum wire. $[(NH_3)_6Ru]Cl_3$ (57 mV versus NHE) or $[py(NH_3)_5Ru]Cl_3$ (305 mV versus NHE)[22] was used as an internal reference. Potentials are reported vs NHE.

(16) Graves, D. J.; Hodgson, D. K. *J. Am. Chem. Soc.* **1979**, *101*, 5608−12.
(17) Clarke, M. J. *Inorg. Chem.* **1980**, *19*, 1103−4.
(18) Bailey, V. M.; Clarke, M. J. *Inorg. Chem.* **1997**, *36*, 1611−8.
(19) Allen, A. D.; Bottomley, F.; Harris, R. O.; Reinslau, V. P.; Senoff, C. V. *J. Am. Chem. Soc.* **1967**, *89*, 5595−9.
(20) Vogt, J. L. H.; Katz, J. L.; Wiberley, S. E. *Inorg. Chem.* **1965**, *4*, 1157−63.
(21) Ford, P.; Rudd, d. F. P.; Gaunder, R.; Taube, H. *J. Am. Chem. Soc.* **1968**, *90*, 1187−94.
(22) Lim, H. S.; Barclay, D. J.; Anson, F. C. *Inorg. Chem.* **1972**, *11*, 1460−6.

Table 1. pK_a's for $[L(NH_3)_5Ru^{III}]^{n+}$ and $[L(NH_3)_5Ru^{II}]^{n+}$ Determined Spectrophotometrically, by ^{1}H NMR, and Electrochemically

			pK_a				
ligand	rotamer	ionization site	Ru^{III} [a]	Ru^{III} [b]	Ru^{III} [c]	Ru^{II}	free ligand
ICytκ^{N2}	N3	N3	2.78 ± 0.01				4.01[d]
ICytκ^{N2}	N1	N1			4.07 ± 0.05	5.28 ± 0.06[c]	
(ICytκ^{N2})$^-$	N1	N3			~10.6		
(ICytκ^{N2})$^-$	N3	N1	9.98 ± 0.01	~10.2	9.38 ± 0.06		9.42[d]
6MeICytκ^{N2}	N3	N3	3.06 ± 0.01			5.2 ± 0.2[c]	
6MeICytκ^{N2}	N1	N1			2.05 ± 0.07	3.28 ± 0.05[c]	
(6MeICytκ^{N2})$^-$	N1	N3		~10.2	11.5 ± 0.6		
(6MeICytκ^{N2})$^-$	N3	N1	10.21 ± 0.02	10.71 ± 0.08	10.36 ± 0.05		
Cydκ^{N4}	N3	N3	3.15[f]	2.61[g]			
(Cydκ^{N4})$^-$	C5	N3		5.27[g]			
5′CMPκ^{N4}	N3	N3	3.60	3.3[g]			
(5′CMPκ^{N4})$^-$	C5	N3		5.0[g]			
(2AmPymHκ^{N1})$^+$						1.79 ± 0.05 2.0 ± 0.2	3.66[e]
2AmPymκ^{N1}		N3			9.1 ± 0.1[g]		
2AmPymκ^{N2}		N1	4.94 ± 0.04		4.9 ± 0.5	~8.5	
$PymH^+$						−0.18 ± 0.01	

[a] Determined spectrophotometrically. pK_a values determined by UV−vis spectroscopy do not discriminate between rotamers. Values presented are expected to Boltzmann-weighted averages, but are listed under the predominant form. [b] Determined by ^{1}H NMR. [c] Determined electrochemically. Values for the 2AmPym complexes are averaged from SW and DPP determinations. [d] Reference 29, 50% ionized from each site. [e] Reference 34. [f] Cyd = cytidine. 1MeCyt = 1-methylcytosine, 5′CMP = 5′-cytidine monophosphate′, see reference 8. [g] Reference 18.

pK_a Determinations. Proton ionization constants were determined by spectrophotometric and NMR titrations and from plots of reduction potential versus pH (Pourbaix plots). Spectrophotometric pK_a values were determined using regression analysis with the equation $pK_a = pH - \log[(A_b - A_{pH})/(A_{pH} - A_a)]$, where A_b is the absorbance of the deprotonated form of the complex, A_a is that for the acidic form, and A_{pH} is the net absorbance at a given pH. Where the fully protonated form was not available, the pK_a was determined as the slope of plots of A_{pH} versus $(A_{pH} - A°)/[H^+]$, where A_{pH} is the absorbance at a given pH and $A°$ is the absorbance of the conjugate base form of the complex. NMR shifts as a function of pH were obtained by manipulating the pH with dilute solutions of DCl and NaOD. These data were fitted to the following equation: $pK_a = pH - \log[(\delta_b - \delta_{pH})/(\delta_{pH} - \delta_a)]$, where δ_b is the chemical shift of the deprotonated form of the complex, δ_a is that for the acidic form, and δ_{pH} is the chemical shift at a given pH. Data for Pourbaix diagrams were obtained by adjusting the pH of the solution with 0.1 M HCl and 0.1 M LiOH, which was internally referenced to the potential of $[py(NH_3)_5Ru]^{3+,2+}$. The potential versus pH plots for $[(ICyt\kappa^{N2})(NH_3)_5Ru^{III,II}]$, $[(6MeICyt\kappa^{N2})(NH_3)_5Ru^{III,II}]$, and $[(2AmPym\kappa^{N1})(NH_3)_5Ru^{III,II}]$ were fitted by standard nonlinear regression methods to $E_h = E^f - 0.591 \log\{([H^+] + K^{III})/([H^+] + K^{II})\}$, where E^f is the formal reduction potential, K^{III} is the ionization constant for the Ru^{III} complex, and K^{II} is that for the corresponding Ru^{II} species.

Kinetics. The rates of rotamerization were obtained using the equation $k = 1/\tau' = [2\pi^2(\Delta\delta_0^2 - \Delta\delta^2)]^{1/2}$, and at coalescence of the two peaks $k = 1/\tau' = 1.41\pi(\Delta\delta)$,[23,24] where $\Delta\delta_0$ is the separation of peaks in the stopped exchange region and $\Delta\delta$ is the separation of peaks in the intermediate exchange region. Ahrennius and Eyring plots of the resulting rate data as a function of temperature yielded the activation parameters. In the case of $[(2AmPym\kappa^{N2})(NH_3)_5Ru]^{3+}$, $\Delta\delta_0$ was estimated from the linearity of the Eyring plot.

The rate of linkage isomerization between $[(2AmPym\kappa^{N2})(NH_3)_5Ru^{III}]^{2+}$ and $[(2AmPym\kappa^{N1})(NH_3)_5Ru^{II}]^{2+}$ was determined by varying the square wave voltammetric scan rate and fitting the resulting relative current peaks by a computer simulation method.[25] Electrochemical kinetic samples were used directly after elution from a CM-Sephadex FF ion exchange column eluted with 0.2 M ammonium formate.

Hydrolysis of $[(2AmPym\kappa^{N1})(NH_3)_5Ru]^{2+}$ was monitored spectrophotometrically at 500 nm under argon at $\mu = 1.0$ and 25 °C. Semilog plots were linear over at least three half-lives. Isosbestic points occurred at 270, 305, and 410 nm at pH 1.6. The plot of k_{obs} versus $[H^+]$ was fitted to the function given in Results using a standard nonlinear least squares technique.

Results

Spectra. The spectrophotometric properties of $[L(NH_3)_5Ru]^{3+}$, where L = ICyt, 6MeICyt, and 2AmPym complexes, are summarized in Table S1 (Supporting Information). In general, the Ru^{III} compounds exhibited a broad ligand to metal charge transfer (LMCT) absorption band between 460 and 560 nm, and a second band at ~300 nm, which is indicative of coordination to an exocyclic amine. An intense absorption in the ultraviolet region was attributed to a $\pi-\pi^*$ ligand absorption. The pK_a's of the complexes measured by various methods are summarized in Table 1. In anticipation of arguments made in the discussion, the first proton ionization (pK_{a1}) from the isocytosine complexes is assigned to N3 of the neutral-ligand complex, while the second (pK_{a2}) is for deprotonation of N1 from the anionic ligand.

^{1}H NMR shifts for the isocytosine complexes as a function of pH are tabulated in Table S2 (Supporting Information). At pH < pK_{a1} of the isocytosine complexes, only one peak is evident, which is attributed to the CH_3 in the 6MeICyt complex and the H6 in the ICyt complex. At pH's between the two pK_a's (pK_{a1} < pH < pK_{a2}), each complex exhibits two additional peaks. One of these arises from the same proton evident at lower pH (H6 with ICyt and CH_3 in 6MeICyt), which is attributed to the presence of a second rotamer. The two rotamers (R_{N1} and R_{N3}) arise from hydrogen-bonding and electrostatic interactions between the $(NH_3)_5Ru^{III}$ moiety and N1 or N3, respectively. In both cases, the lower-intensity peak was also somewhat broader. Since in R_{N1} the paramagnetic center is closer to C6, this rotamer was assigned to the broader, less intense signal. A second new peak in the mid-pH range is attributed to H5 in both complexes, which becomes observable because the rotation of the paramagnetic metal ion around the N−C6 bond is slowed by the hydrogen-bonding and electrostatic interactions to the ring nitrogens. At pH > pK_{a2}, only a single peak was again evident,

(23) Macomber, R. S. *A Complete Introduction to Modern NMR Spectroscopy*; Wiley and Sons: New York, 1998; pp 158−72.
(24) Drago, R. S. *Physical Methods for Chemists*, 2nd ed.; Saunders College Publishing: Ft. Worth, 1992.
(25) Tracey, A. A.; Eriks, K.; Prock, A.; Giering, W. P. *Organometallics* **1990**, *9*, 1399−405.

Table 2. Rate Constants at 30 °C and Activation Parameters for Rotation around the C−N Bond in Exocyclically Coordinated Complexes, $[L(NH_3)_5Ru^{III}]^{n+}$

ligand	k (s^{-1})	ΔH* (kcal/mol)	ΔS* (cal/mol K)
$(ICyt\kappa^{N2})^-$	2.9×10^3	2.7 ± 0.1	-34 ± 1
$(6MeICyt\kappa^{N2})^-$	3.6×10^3	1.6 ± 0.1	-37 ± 1
$2AmPym\kappa^{N2}$	5.8×10^3	1.5 ± 0.1	-37 ± 2

which is assigned to the CH_3 and the H6, in 6MeICyt and ICyt complexes, respectively. In the case of $[(2AmPym\kappa^{N2})(NH_3)_5Ru^{III}]^{3+}$ separate H4 and H6 resonances were observed in the neutral ligand complex (shown in Figure 2), which contains a single protonated ring nitrogen. As with the isocytosine ligands, when this proton was removed, so that the metal center could hydrogen bond to either ring nitrogen, only a single (average) resonance was observed for H4 and H6.

For the rotameric kinetic study, the ^1H NMR signals of $ICyt^-$, $6MeICyt^-$, and 2AmPym (see Figure S1, Supporting Information) complexes were monitored at a pH such that both rotamers were evident and the temperature was increased in 10 °C increments until coalescence of the resonances attributed to the two rotameric forms was observed. Rotameric rate constants at 30 °C and activation parameters for the complexes with the anionic ligands $(ICyt^-\kappa^{N2})^-$ and $(6MeICyt^-\kappa^{N2})^-$ and the neutral ligand $2AmPym\kappa^{N2}$ are comparable (cf. Table 2). All rate constants (Table S3) and the Eyring plots (Figure S2) are given in the Supporting Information.

Electrochemistry. Reduction potentials for the exocyclically and endocyclically coordinated complexes are summarized in Tables 3, sections a and b, respectively. Investigation of the exocyclic-Ru^{III} forms of the complexes by cyclic voltammetry (CV) revealed an irreversible peak on the initial cathodic scan at a potential around 0 V. For the isocytosine complexes, this cathodic wave exhibited broadening or a shoulder in the pH range between pK_{a1} and pK_{a2}. Subsequent scans revealed an additional, reversible peak around 200 mV, which is attributed to the endocyclically coordinated form. In general, cyclic voltammetric scans for the endocyclic complexes appeared both chemically and electrochemically reversible at scan rates greater than 100 mV/s between pH 2 and 10 (see Figure S3, Supporting Information). Those for the exocyclically coordinated complexes were chemically irreversible at the scan rates employed (Figure S3).

Current peak shapes in square wave voltammetry were similar to the internal standard, and were identical on carbon paste, platinum, and glassy carbon electrodes with no obvious indication of adsorption. In the square wave voltammograms of the 6MeICyt and the ICyt complexes, only one peak was evident on scanning negatively at pH < pK_{a1}. However, on scanning anodically from a potential below this wave, a new peak was evident around 0.1−0.15 V (vs NHE). Cathodic scans, in the pH range pK_{a2} < pH < pK_{a1}, yielded a distinct shoulder separated by about 0.2 V from the larger peak. Figure 3 shows the pH dependence of these two reduction potentials for the isocytosine complexes.

Cyclic voltammetry of $[(2AmPym\kappa^{N1})(NH_3)_5Ru^{II}]^{2+}$ showed a reversible peak at about 0.35 V. The CV of $[(2AmPym\kappa^{N2})(NH_3)_5Ru^{III}]^{2+}$ was similar to that described for the isocytosine complexes, except that the new peak attributed to the endocyclic form occurred at a more cathodic potential.

Pourbaix plots for the exocyclic isocytosine complexes are shown in Figure 3, and those for both the exocyclic and endocyclic forms of $[(2AmPym)(NH_3)_5Ru^{II/III}]$ are shown in Figure 4. In the case of $[(2AmPym\kappa^{N2})(NH_3)_5Ru^{II/III}]$, these

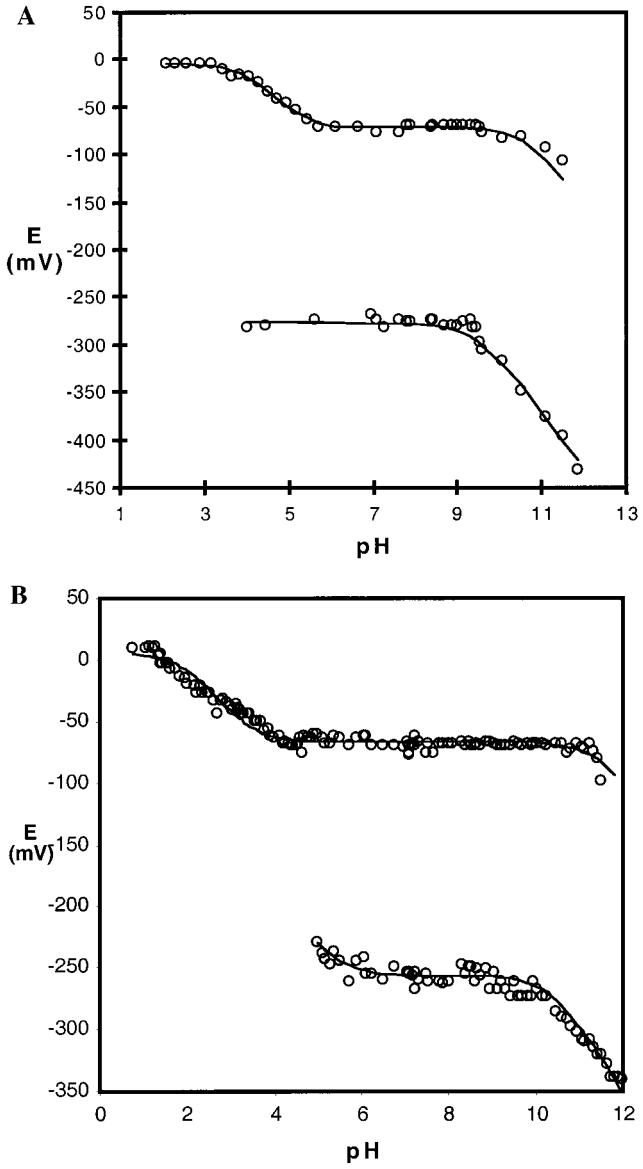

Figure 3. Pourbaix diagrams for (A) $[ICyt\kappa^{N2}(NH_3)_5Ru]^{3+}$ and (B) $[6MeICyt\kappa^{N2}(NH_3)_5Ru]^{3+}$ in 0.1 M LiCl at 23 °C. In both cases the upper curve is assigned to the rotamer in which the metal ion is hydrogen bonded to N1 (R_{N1}), while the lower is attributed to the metal ion's being on the N3 side (R_{N3}). Fitted parameters are given in Tables 1 and 2.

studies were carried out by both square wave voltammetry and differential pulse polarography in order to clarify the change in slope at pH > 8. The data illustrated in Figure 4a also suggest a pK_a of ~2 for $[(2AmPymH\kappa^{N2})^+(NH_3)_5Ru^{II}]^{3+}$.

Computer simulation[25] of the relative peak heights of currents attributed to $[(2AmPym\kappa^{N2})(NH_3)_5Ru]^{3+/2+}$ and $[(2AmPym\kappa^{N1})(NH_3)_5Ru]^{3+/2+}$ in solutions of $[(2AmPym\kappa^{N2})(NH_3)_5Ru^{III}]^{3+}$ at various square wave voltammetric scan rates between 80 and 120 mV/s (pH 3, $\mu = 0.1$, 23 °C) yielded a rate constant of 3.9 ± 0.6 s^{-1} for the ECE reaction (see Figure S4, Supporting Information):

$$[(2AmPym\kappa^{N2})(NH_3)_5Ru]^{3+} + e^- \rightarrow$$
$$[(2AmPym\kappa^{N2})(NH_3)_5Ru]^{2+} \rightarrow [(2AmPym\kappa^{N1})(NH_3)_5Ru]^{2+}$$

Hydrolysis of $[(2AmPym^{\kappa 1})(NH_3)_5Ru]^{2+}$. The hydrolysis of $[(2AmPym\kappa^{N1})(NH_3)_5Ru]^{2+}$ was first-order in the complex. The

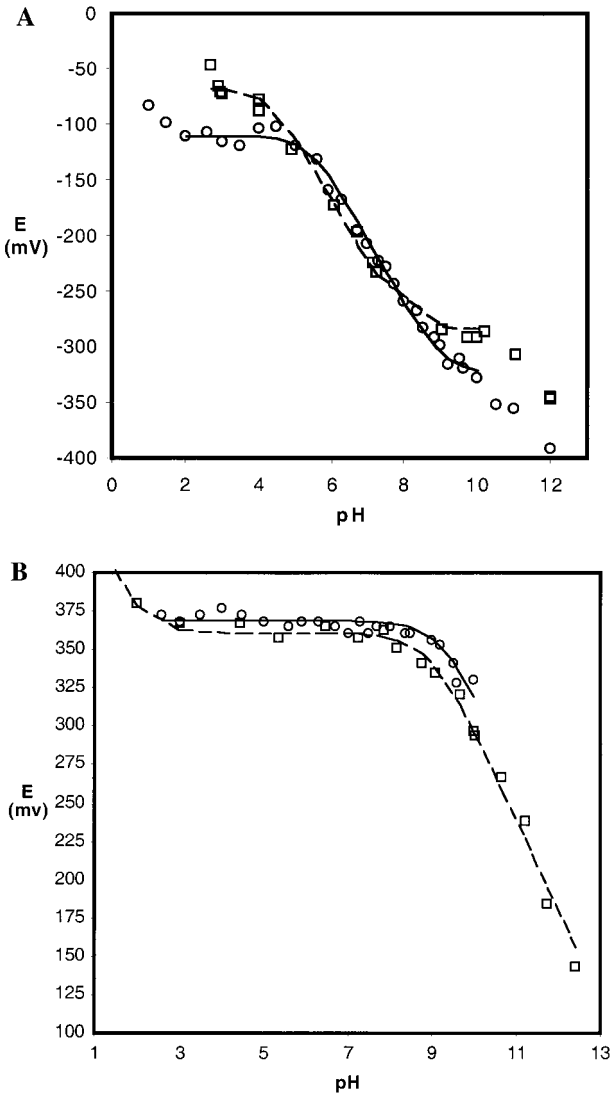

Figure 4. Pourbaix diagrams (vs NHE): (A) $[2AmPym\kappa^{N2}(NH_3)_5Ru]^{3+}$ in 0.1 M LiCl at 23 °C by square wave volatammetry (circles) and differential pulse polarography (squares). The solid line shows the fit to the equation $E = E° - 59 \log\{([H^+] + K_a^{III})/([H^+] + K_a^{II})\}$ over the range of data used. For SW and DPP, respectively, the least-squares fits yielded the following: $E°$ (mV), -110 ± 3 and -66 ± 10; pK_a^{III}, 5.41 ± 0.06 and 4.3 ± 0.3; pK_a^{II}, 9.0 ± 0.1 and 8.0 ± 0.3. Averaged parameters are given in Tables 1 and 2. (B) $[2AmPym\kappa^{N1}(NH_3)_5Ru]^{3+}$, same as for A except that the equation $E = E° - 59 \log\{([H^+] + K_a^{III})/[H^+]\}$ was used. For SW and DPP, respectively, the least-squares fits yielded the following: $E°$ (mV), 369 ± 4 and 361 ± 5; pK_a^{III}, 9.23 ± 0.07 and 8.94 ± 0.1. The DPP data also yielded a value for pK_a^{II}, 2.0 ± 0.2. Averaged parameters are given in Tables 1 and 2.

observed rate constants plotted in Figure 5 as a function of pH were fitted to the equation

$$k_{obs} = \frac{k_1[H^+] + k_0K_1}{[H^+] + K_1}$$

where $K_a = (8.8 \pm 0.3) \times 10^{-2}$, $k_0 = (1.7 \pm 0.2) \times 10^{-4}$ s^{-1}, and $k_1 = (3.01 \pm 0.06) \times 10^{-3}$ M^{-1} s^{-1}. Attempts to observe the hydrolysis of the corresponding pyrimidine complex, $[(Pym)(NH_3)_5Ru]^{2+}$,[21] revealed that it was stable in 1 M acid for up to 3 days in the absence of light. The kinetic pK_a of 2.06 ± 0.07 is in reasonable agreement with the spectrophotometrically determined value of 1.79 ± 0.05.

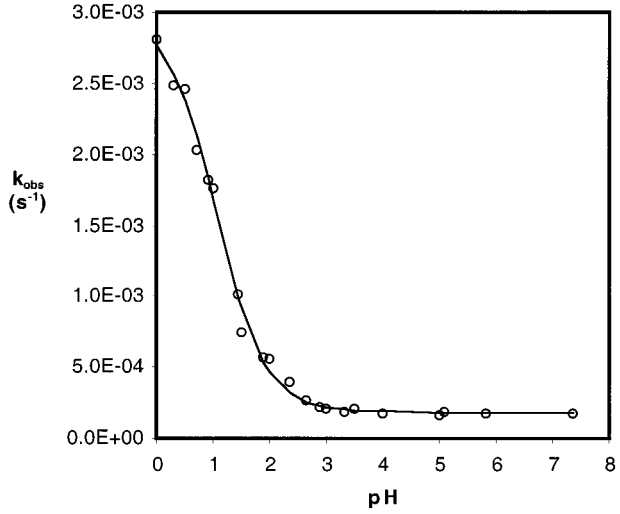

Figure 5. Plot of k_{obs} for the hydrolysis of $[2AmPym(NH_3)_5Ru]$ as a function of pH. Data were fitted to $k_{obs} = (k_0K_a + k_1[H^+])/(K_a + [H^+])$, where $K_a = (8.8 \pm 0.3) \times 10^{-2}$, $k_0 = (1.7 \pm 0.2) \times 10^{-4}$ s^{-1}, $k_1 = (3.01 \pm 0.06) \times 10^{-3}$ M^{-1} s^{-1}.

MO Energy Calculations. ZINDO (INDO/1) calculations were performed on a CAChe workstation.[26,27] AM1, MNDO, MNDO/3, and PM3 calculations were done in Chem3D.[28]

Discussion

Structure. The previously reported crystal structure of the analogous cytosine complex, $[1MeCyt\kappa^{N6}(NH_3)_5Ru](PF_6)_2$, revealed that the metal center was coordinated to the ionized exocyclic nitrogen.[16] The UV−vis and ^{1}H NMR spectra of the complexes presented here, coupled with their electrochemical and acid−base behavior, are consistent with the distinctive properties evident with exocyclic amine coordination (Tables 1S and 2S).[8,18] These complexes exhibit a strong absorption in the 300−400 nm region in the near UV, which is almost diagnostic for coordination of $(NH_3)_5Ru^{III}$ to an exocyclic amine versus endocyclic imine.[8] Also, the reduction potentials (∼−0.07 V) of the complexes reported here are low for heterocyclic imine nitrogen coordination of pentaammineruthenium(III) complexes, but are consistent with exocyclic amido binding (cf. Table 2).[8] Finally, the ^{1}H NMR spectra are analogous to those of $[L(NH_3)_5Ru^{III}]$, where L = cytosine and adenine coordinated at the exocyclic nitrogen.[18]

The pK_{a1} values of ∼3 in the ICyt complexes (Table 1) are consistent with displacement of a proton from an exocyclic amine to a ring imine nitrogen.[8] The more acidic ionization, pK_{a1}, probably represents loss of a proton preferentially at N3, but in equilibrium with the N1 tautomeric and rotameric forms (see Figures 6 and S5, Supporting Information). The N3-ionized form should be stabilized not only by ammine-N3 hydrogen bonding but also by the stronger electrostatic interactions between Ru^{III} and the anionic charge resident on the oxygen in several canonical forms (Figure S3). INDO/1 molecular orbital calculations indicate stabilization of the N3 deprotonated form by an anionic charge on the oxygen of 0.025 formal charge units. The differences in pK_{a2} values between the two rotameric forms (see Table 1, $\Delta pK_{a2} = 1.2$ for both the $ICyt^-$ and

(26) Anderson, W. P.; Cundari, T. R.; Drago, R. S.; Zerner, M. C. *Inorg. Chem.* **1990**, *29*, 1−3.
(27) CAChe Scientific, Inc., CAChe 1994, TekGraphics, Beverton, OR.
(28) Rubenstein, M.; Rubenstein, S. *Chem3D Pro*, 3.51 ed.; Cambridge Scientific Computing, Inc.: Cambridge, MA, 1997.

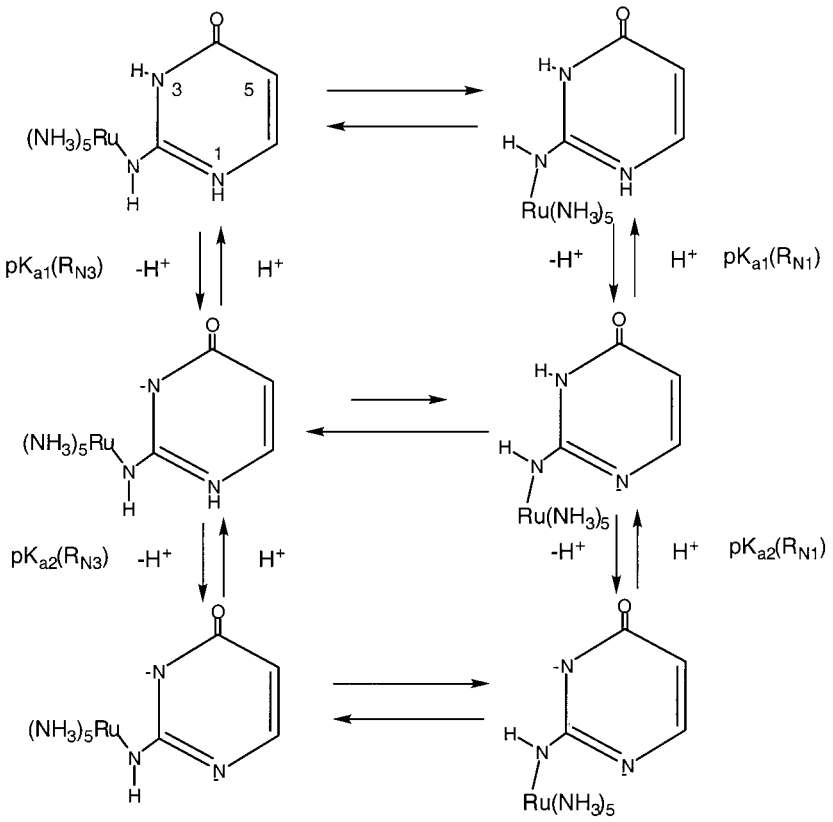

Figure 6. Rotameric, tautomeric, and ionization equilibria of $[ICyt\kappa^{N2}(NH_3)_5Ru^{III}]^{3+}$.

6MeICyt$^-$ complexes, respectively, estimated electrochemically) indicate that ionization is favored at N1 by 1.6 kcal, when the Ru^{III} is on the N1 side (R_{N1}) and available to hydrogen bond to the ionized N1, rather than already hydrogen bonded to N3 (R_{N3}). While R_{N3} is more stable on ICyt$^-$, R_{N1} is possible as the *cis*-ammine ligands may straddle the protonated ring nitrogen, HN1.

The difference in acidities ($\Delta pK_a = 2.0$) between $[(2AmPymH\kappa^{N1})^+(NH_3)_5Ru^{II}]^{3+}$ and $[(PymH^+)(NH_3)_5Ru^{II}]^{3+}$ (see Table 1) reflect those of the free ligands ($\Delta pK_a = 2.4$) and can be attributed to the electron donor effect of the amino group. In contrast, the great increase in acidity of $[(2AmPym\kappa^{N2})(NH_3)_5Ru^{III}]^{3+}$ relative to that of the neutral free ligand is due not only to the presence of the tripositive metal ion but also to the displacement of the proton from the much more basic amine to the adjacent ring imine.

Unlike the corresponding cytidineκ^{N4} (Cyd) and 5′-cytidineκ^{N4} monophosphate (5′CMP) complexes, which exhibit separate rotameric NMR signals near their pK_a's, the rotamers of the neutral ligand isocytosineκ^{N2} complexes did not yield separate NMR signals, so that the pK_a's of the two rotameric forms could not be determined (cf. Table 1).

Linkage Isomerization. The new current peaks occurring at 0.1−0.15 V (vs NHE) at pH < pK_{a1} following the reduction of the Ru^{III} complexes of ICytκ^{N2} and 6MeICytκ^{N2} can be attributed to linkage isomerization of the electrochemically formed Ru^{II} to N1 (see Table 3b). This behavior is also evident in the electrochemistry of the analogous 2-aminopyrimidineκ^{N2} (see Figure 2) and has been reported previously for a number of adenine$^{\kappa 6}$ complexes. The rate constant (3.9 s^{-1}) for the $\kappa^{N2} \rightarrow \kappa^{N1}$ forms of $[(2AmPym)(NH_3)_5Ru]^{2+}$ indicates the facility of this reaction in an ECE mechanism following reduction of $[(2AmPym\kappa^{N2})(NH_3)_5Ru^{III}]^{3+}$ (Figures S3 and S4) and is consistent with those ($\sim$10 s^{-1}) seen in a similar system involving the movement of $(NH_3)_5Ru^{II}$ from the amido nitrogen of picolinamides to the pyridine nitrogen.[12]

In these species, the electrochemically produced Ru^{II} cannot enter into π-bonding with the exocyclic amine, but is ideally situated to migrate to an adjacent imine nitrogen, where it can form a $d_\pi \rightarrow \pi^*$ back-bond with the pyrimidine ring. Consistent with this linkage isomerization not being observed in the analogous cytidine complexes,[8] N3 is sufficiently sterically hindered by both the oxygen and exocyclic amine to prevent firm binding. Consequently, the ring-bound form is assigned to N1 coordination for both ICyt and 6MeICyt.

The lower $Ru^{III,II}$ potential, when the metal ion is on ICytκ^{N1} compared to 2AmPymκ^{N1} (cf. Table 2b), is attributed to resonance forms of the former that place an anionic charge on the lone pair nitrogen (see Figure S5). Calculations by several methods (AM1, MNDO, MNDO/3, PM3)[28] indicate an increase in anionic charge on the lone pair nitrogen by about 0.05 units in ICyt relative to 2AmPym. In comparison with 2AmPymκ^{N1}, such an increase in electron density at the bonding nitrogen should stabilize Ru^{III} on electrostatic grounds and destabilize Ru^{II} by inhibiting $d_\pi \rightarrow \pi^*$ back-bonding into the pyrimidine. The transient stability of the Ru^{II} N1-bound forms of the isocytosine complexes is probably due to (1) steric hindrance provided by the exocyclic ammine (N2), (2) decreased back-bonding, and (3) possibly an acid hydrolytic mechanism similar to that indicated below for $[(2AmPym\kappa^{N1})(NH_3)_5Ru]^{2+}$.

Rotamerization. The difference in reduction potentials for the two ionized rotamers (Figure 3a) indicates that R_{N3} is 4.7 and 4.4 kcal (ICyt and 6MeICyt, respectively) more stable and, therefore, more difficult to reduce, since the Ru^{III} is closer to the anionic oxygen. The more broadened of the two ^1H NMR signals that occur at pK_{a1} < pH < pK_{a2} for H6 and CH_3(6) in the ICyt and 6MeICyt, complexes, respectively, is attributed to R_{N1}, since this places the paramagnetic center closer to C6.

Integration of the methyl proton NMR peaks in the 6MeICyt$^-$ complex yields an estimate of $K = [R_{N3}]/[R_{N1}]$ of 4.5, indicating that R_{N3} is about 1 kcal/mol more stable than R_{N1} on the monodeprotonated ligands. The presence of more than one ^{1}H NMR resonance (see Figure S1 and Table S2) for the same protons and the observation of two voltammetric waveforms (Figure 3) indicate that more than one species is present in solution when $pK_{a1} < pH < pK_{a2}$ for both isocytosine complexes. Prior reduction of the isocytosine complexes resulted in more equal current peaks for the two rotamers upon anodic scans, but with the more negative peak, which is attributed to R_{N3}, remaining larger.

While the N1 and N3 tautomers of the neutral isocytosine free ligand exist in equal quantities in aqueous solution,[29] the ^{1}H NMR of the metal complex (at $pK_{a1} < pH < pK_{a2}$) indicates a higher concentration of one form. A hydrogen bond between a coordinated amine and an anionic ring nitrogen should retard the tautomerization between the N1 and N3 sites. Consequently, at pH values midway between the two pK_a's two distinct resonances are observed for both H6 in the ICyt complex and the methyl group in the case of 6MeICyt. Below this pH range, hydrogen bonding cannot occur to either N1 or N3, so neither rotamer is stable on the NMR or electrochemical time scales and only a single, average peak is observed for protons around C6. The rotation of the paramagnetic center around the N2−C2 axis at low pH should result in a strong oscillation of both the dipolar paramagnetic field and the spin density transmitted by changes in $\pi-d_\pi$ overlap to the para position. Consequently, a very short NMR relaxation time (t_1) is expected for H5, which results in so severe a broadening of the H5 resonance that it becomes unobservable. A similar effect occurs at $pH > pK_{a2}$, where $[(NH_3)_5Ru]^{3+}$ may hydrogen bond to either adjacent ring nitrogen, with localization on either being short on the NMR time scale, but not on the electrochemical time scale.

Consistent with the NMR results at $pH < pK_{a1}$, the voltammetry of $[6MeICyt(NH_3)_5Ru^{III/II}]$ exhibits only a single peak on the cathodic scan, since $[(NH_3)_5Ru]^{3+}$ is unable to stabilize its position by hydrogen bonding to either H−N1 or H−N3. However, at $pK_{a1} < pH < pK_{a2}$ scanning negatively, a second peak appears. The peak with the more negative potential is assigned to the N3 rotamer, since the closer proximity of the metal ion to the anionic site should make it more difficult to reduce. The first ionization site is similarly assigned as N3 because of the stronger electrostatic interaction between the N3 hydrogen bonded rotamer and the anionic charge localized on O4. Both voltammetric peaks are consistent in that they move to more negative potentials with increasing pH. On scanning positively, the R_{N1} form becomes evident at a pH almost one unit higher because of the decreased electrostatic effect of the Ru^{II} ion.

Kinetics of Rotamerization. Due to conjugation of the nitrogen lone pair with the aromatic ring, the C−NH_2 bond in heteroaromatic amines usually exhibits partial double bond character, which gives rise to a π-barrier to rotation.[1,30] The difference in rotational rate constants at room temperature between 1MeCyt (1.38×10^2 s^{-1})[31] and the complexes reported here (3.15×10^3 s^{-1} for $[(6MeICyt^-)\kappa^{N2}(NH_3)_5Ru]^{2+}$) indicates that the Ru^{III} significantly lowers the barrier to rotation. While the rotational kinetics are rapid, the large paramagnetic shifts provide a large $\Delta\delta$, which allows the reaction to be monitored.

Table 3. Reduction Potentials of Exocyclically and Endocyclically Coordinated Complexes $[L(NH_3)_5Ru^{III}]^{n+}$

(a) Reduction Potentials[a] of Exocyclically Coordinated Complexes

ligand	rotamer	ionized site	$E°$ (mV)
ICytκ^{N2}			8
(ICytκ^{N2})$^-$	N1	N3	−70
(ICytκ^{N2})$^{2-}$	N3	N1	−276
6MeICytκ^{N2}			7
(6MeICytκ^{N2})$^-$	N1	N1	−67
(6MeICytκ^{N2})$^{2-}$	N3	N3	−256
Cydκ^{N4}			9
(Cydκ^{N4})$^-$	C5	N3	−300
2AmPymκ^{N2}			−88
(2AmPymκ^{N2})$^-$	N1	N1	∼−275

(b) Reduction Potentials[b] of Endocyclically Coordinated Complexes

ligand	$E°$ (mV)
ICytκ^{N1}	140
6MeICytκ^{N1}	100
2AmPymκ^{N1}	365
Pymκ^{N1}	427

[a] Relative to NHE. [b] Versus NHE. Measured by anodic square wave voltammetric scan at $\mu = 0.1$, pH 2−3.

While the rotameric movements in these complexes have small activation energies (cf. Table 2), the large, negative ΔS^* values suggest a highly structured transition state. The rotational barrier for an analogous heterocycle, 1,7,7-trimethylcytosine, when measured by an NMR line shape technique is $\Delta H^* = 15.2$ kcal/mol ($\Delta S^* = 0.2$ cal/mol K, and $E_a = 15.7$ kcal/mol).[1] Since the steric hindrance presented by $(NH_3)_5Ru-NH-$ is no less than that of $(CH_3)_3N-$, the difference in the activation barriers to rotation either is electronic or has to do with the displacement of the exocyclic proton to an adjacent ring imine. Ionization of the exocyclic amine would normally be expected to increase π_N donation into the ring with concomitant increases in π-bonding and the barrier to rotation. Since Ru^{III} is a π-electron acceptor that also interacts with the π lone pair of the exocyclic nitrogen, the Ru−N partial double bond forms at the expense of the C−N π-bond. Consequently, the barrier to rotation decreases by more than 10 kcal/mol, relative to the free ligand. The slightly lower activation barrier for the complex with 6MeICyt relative to that with ICyt (Table 3) is consistent with earlier studies on the free ligands showing that the electron-donating methyl substituent in non-ortho positions lowers the barrier to rotation by decreasing the C−N partial double bond.[1]

Perhaps owing to the decrease in the C−N π-bonding caused by Ru^{III}, the ring imine proton adjacent to the exocyclic amine may be responsible for much of the activation barrier. Distinct rotameric NMR signals were observed only in pH ranges where a single ring imine proton was present, regardless of whether the ligand was anionic (1MeICyt$^-$ or 6MeICyt$^-$) or neutral (2AmPym). The relatively large negative values for ΔS^* (Table 3) suggest a highly structured transition state, which may derive partly from *cis*-ammines being sterically hindered from rotating when straddling an adjacent heterocyclic −NH.

In previously reported complexes of adenosineκ^{N6}, cytidineκ^{N4}, and 1-methylcytosineκ^{N6},[8,18] where tautomerization between the ring nitrogens is not possible, the proton serves as a switch controlling the conformation, thereby providing for atropisomerism. In the present complexes, the rate may be limited by either proton tautomerization or the π-barrier to rotation of the metal center.

(29) Kwiatkowski, J. S.; Pullman, B. In *Advances in Heterocyclic Chemistry*; Katritzky, A. R., Boulton, A. J., Eds.; Academic Press Inc.: New York, 1975; Vol. 18, pp 316−7.
(30) Gallo, R.; Roussel, C.; Berg, U. *Steric Effects in Heteroaromatics*; Academic Press: New York, 1988; Vol. 43, pp 241−6.
(31) Shoup, R. R.; Becker, E. D.; Miles, H. T. *Biochem. Biophys. Res. Commun.* **1971**, *43*, 1350−3.

Hydrolysis of [(2AmPymκ^{N1})$(NH_3)_5$Ru]$^{2+}$. The hydrolytic instability of [(2AmPymκ^{N1})$(NH_3)_5$Ru]$^{2+}$ relative to the corresponding pyrimidine complex indicates that the exocyclic amino group plays a special role in the dissociation of the complex. The π-donor properties of the amine inhibit metal-to-ligand, $d_\pi \rightarrow \pi^*$ back-bonding so as to destabilize Ru^{II}, which is indicated by a 5 nm shift to higher energy in the metal-to-ligand charge transfer transition relative to the analogous pyrimidine complex.[21] The π-donor interaction also increases heterocyclic $\pi \rightarrow d_\pi$ bonding, which stabilizes Ru^{III}. This is confirmed by the decrease in $E°$ between the Pym (427 mV) and 2AmPym (350 mV) complexes. The lower reduction potential also explains why the 2AmPym complex undergoes air oxidation much more rapidly than the pyrimidine complex. Second, space-filling models show some steric strain produced by the amine protons impinging on the metal center, which would tend to weaken the metal−pyrimidine bond. The decreased back-bonding and steric hindrance generated by the amine group partially account for the greater dissociation rate of the 2AmPymκ^{N1} complex relative to the fairly stable pyrimidine complex. The analogous 4-aminopyridine complex is also acid labile, which may have to do with ease of protonation of the ligand or the metal ion to produce a labile intermediate.[32]

The steric repulsion between 2AmPymκ^{N1} and [$(NH_3)_5$Ru] is minimized when an amine proton sits on an octahedral face of the metal ion. This geometry probably explains much of the acid lability of the 2AmPymκ^{N1} complex, which is in marked contrast to the stability of the pyrimidine complex. The plot of k_{obs} versus pH in Figure 5 indicates a protonated species, which forms near the thermodynamic pK_a (cf. Table 1) and dissociates much more rapidly than the neutral-ligand complex. While both pyrimidine and 2AmPymκ^{N1} accept a proton at the free ring nitrogen (N3), which increases back-bonding from the metal, there is no hydrolytic effect with the former. This may be due to the formation of a 7-coordinate, hydride intermediate, which has long been postulated in the acid-catalyzed hydrolysis of Ru^{II} ammine complexes.[33] The amino group juxtaposed to Ru^{II} in 2AmPymκ^{N1} may facilitate the addition of a proton to the octahedral face of the metal center in a concerted process, whereby the proton added to the imine shifts to the amine as the amine proton transfers to the metal ion. The ease of forming the 7-coordinate hydride transient in this fashion should greatly enhance the rate of ligand dissociation. The combination of decreased back-bonding, steric repulsion, and concerted proton transfer to the metal ion readily accounts for the relative instability and acid-lability of N1-bound complexes with both 2AmPym and adenine,[8] where an exocyclic amine is also adjacent to the metal coordination site.

Acknowledgment. This work was supported by PHS Grant GM26390. We are grateful to Gary Sardon for help with the electrochemical experiments.

Supporting Information Available: NMR spectra as a function of temperature for [2AmPym$\kappa^{N2}$$(NH_3)_5$$Ru^{III}$]$^{2+}$. Eyring plots for the rotamerization of [ICyt$\kappa^{N2}$$(NH_3)_5$$Ru^{III}$]$^{2+}$, [6MeCyt$\kappa^{N2}$$(NH_3)_5$$Ru^{III}$]$^{2+}$, and [2AmPym$\kappa^{N2}$$(NH_3)_5$$Ru^{III}$]$^{2+}$; experimental and simulated square wave voltammetric scans; rotamers, tautomers, and resonance structures for [ICyt$\kappa^{N2}$$(NH_3)_5$$Ru^{III}$]$^{2+}$. Tables of UV−visible spectral data, ^{1}H NMR resonances, and rotamerization k_{obs} versus temperature. This material is available free of charge via the Internet at http://pubs.acs.org.

IC000512E

(32) Sutton, J. E.; Taube, H. *Inorg. Chem.* **1981**, *20*, 4021−3.
(33) Ford, P. C.; Kuempel, J. R.; Taube, H. *Inorg. Chem.* **1968**, *7*, 1976−83.
(34) Perrin, D. D. *Dissociation constants of organic bases in aqueous solution: Supplement 1*; Butterworth: London, 1972.